

Large deviations in models of growing clusters with symmetry-breaking transitions

Robert L. Jack

*Department of Applied Mathematics and Theoretical Physics, University of Cambridge,
Wilberforce Road, Cambridge CB3 0WA, United Kingdom and*

Department of Chemistry, University of Cambridge, Lensfield Road, Cambridge CB2 1EW, UK

We analyse large deviations of the magnetisation in two models of growing clusters. The models have symmetry-breaking transitions, so the typical magnetisation of a growing cluster may be either positive or negative, with equal probability. For large clusters, the magnetisation obeys a large deviation principle. We show that the corresponding rate function is zero for values of the magnetisation that are intermediate between the two steady state values, which means that fluctuations with these values of the magnetisation are much less unlikely than previously thought. We show that their probabilities decay as power laws in the cluster size, instead of the exponential scaling that would be expected from the large deviation principle. We discuss how this observation is related to dynamical phase coexistence phenomena.

I. INTRODUCTION

Large deviation theory is the mathematical framework for analysis of rare events [1]. In recent years, this theory has been applied to a wide range of physical systems, in order to study dynamical fluctuations [2–11]. In non-equilibrium systems, large-deviation theory can be used to analyse fluctuations of currents and of the entropy production [2–6], with implications for fluctuation theorems [2, 12] and thermodynamic uncertainty principles [13]. In systems that exhibit metastability, including glasses [9, 14, 15] and biomolecules [16], large deviation theory can be used to analyse deviations from ergodic behaviour, generating new insights into long-lived metastable states.

To illustrate the simplest case, consider a system with (time-dependent) state $x(t)$, which follows some stochastic dynamics. Select an observable quantity $F(x)$, and construct its time average as

$$\bar{F}(\tau) = \frac{1}{\tau} \int_0^\tau F(x(t)) dt. \quad (1)$$

This quantity is a random variable. A simple statement of ergodicity is that \bar{F} should converge to a corresponding ensemble average, in the limit where $\tau \rightarrow \infty$. Large deviation theory provides a framework in which this convergence can be analysed [6, 7, 14, 17]. Definitions will be given below, here we give an outline of the physical picture. In simple cases, the probability density for \bar{F} scales for $\tau \rightarrow \infty$ as

$$p(\bar{F}|\tau) \simeq \exp[-\tau I(\bar{F})]. \quad (2)$$

This type of scaling relationship is called a large deviation principle (LDP) and I is called the rate function [1, 18]. For physical systems that are finite and ergodic, one expects that the rate function is (strictly) convex, with a single zero when \bar{F} is equal to the ensemble average.

However, there is a wide range of physical systems where this simple picture breaks down. For example, in systems with long-lived metastable states, it is natural for the rate function to develop singularities [9, 19], which

appear as the system size tends to infinity. Systems with long-ranged memory may also behave non-ergodically, in which case the rate function may not be convex [20, 21].

In this work, we consider systems where clusters of particles grow, as a function of time [22, 23]. The clusters contain two kinds of particles, which can be distinguished either by their spins (up or down), or their colors (red or blue). Using the language of spins, one defines the (extensive) magnetisation, which is the difference between the number of spin-up particles and the number of spin-down particles. We focus here on models that are symmetric under interchange of spin-up and spin-down. In this case, Klymko, Garrahan, and Whitelam [22] showed that these systems exhibit a range of interesting behaviour, including symmetry-breaking transitions. That is, depending on the model parameters, the (intensive) magnetisation can converge to zero at large times, or it can converge to a non-zero value [22]. In the latter case, positive and negative values are equally likely, but typical trajectories of the model involve spontaneous breaking of the up-down symmetry.

Recently [11], Klymko, Geissler, Garrahan and Whitelam (KGGW) analysed LDPs similar to (2), in these growth models. Since the clusters are always growing with time, the models are not ergodic. This means that one cannot apply standard methods from [6, 7, 24] in order to establish LDPs similar to (2). Nevertheless, KGGW showed that an LDP holds at large time, where the observable analogous to \bar{F} is the average magnetisation.

For parameters where the symmetry is spontaneously broken, Ref. [11] also predicted two unusual properties of the rate function. First, there are some values of the observable for which the rate function is concave (the second derivative is negative). Second, in cases where the steady states spontaneously break the symmetry, they predicted that the rate function should have local minima at unstable fixed points of the dynamics. From (2), it follows that these unstable points should be associated with local maxima in the probability, although these maxima were not observed in [11]. These predictions were based on a method that provides upper bounds on the rate func-

tion [11, 25]. This is achieved by modifying the dynamics of the system of interest, in order to make the rare events of interest more likely. A recent preprint [26] discusses this method in more detail, and proposes a method for calculation of the difference between the upper bounds and the true rate functions.

In this work, we examine the LDPs of KGGW in more detail. We find that while their upper bounds on the rate function are valid, these bounds are not quantitative estimates of the rate functions themselves. In particular, we show that the second derivative of the rate function may be zero, but it is never negative. (The rate function is not strictly convex, but neither is it concave.) This also explains why the probability distribution of the magnetisation does not have local maxima at unstable fixed points of the dynamics.

Our analysis also reveals additional interesting and unusual behaviour in these systems. In cases where the symmetry is spontaneously broken, we find that the probability distribution of the magnetisation behaves similarly to (2) for some values of the magnetisation, while for some other values it behaves as a power law $p(\bar{F}|\tau) \simeq \tau^{-\alpha}$. We discuss the physical interpretation of this unusual scaling – it is associated with the fact that very large fluctuations can be observed for trajectories that diverge slowly from the unstable fixed point of the dynamics. In the light of these results, we discuss what general insights are available, including the strengths and weaknesses of numerical strategies for analysis of LDPs. In particular, we emphasise that while upper bounds on rate functions are useful, establishing quantitatively accurate bounds is likely to require a detailed understanding of the system of interest [27–29], or a very flexible variational ansatz [30].

In this paper, Sec. II reviews the definitions of the models and the methods of [11, 22]; this includes a model of irreversible cluster growth, and one where the cluster grows reversibly, so that the number of particles can both increase or decrease. Sec. III has results for the irreversible process, and Sec. IV has results for the reversible process. In Sec. V we discuss what general conclusions can be drawn from our results.

II. MODELS AND METHODS

A. Irreversible model of growth

We first consider a model where clusters grow irreversibly [22], see also [23]. This is a stochastic process in discrete time. Let $s_k = \pm 1$ be spin of the particle that is added on step k . The (intensive) magnetisation just after this step is

$$m_k = \frac{1}{k} \sum_{i=1}^k s_i. \quad (3)$$

The initial condition is that $s_1 = \pm 1$, each with probability 1/2. The dynamical rule is that

$$s_{k+1} = \begin{cases} +1, & \text{with prob } (1 + \exp(-2Jm_k))^{-1}, \\ -1, & \text{with prob } (1 + \exp(2Jm_k))^{-1}. \end{cases} \quad (4)$$

The parameter $J > 0$ describes a ferromagnetic interaction among the spins.

There are several possible ways to analyse this growth process. It can be interpreted as a Markov process for m_k , in which the transition probabilities depend explicitly on the step k . (The process is not stationary.) Alternatively, the system can be viewed as a non-Markovian process for s_k , in which the transition probabilities depend on the history, via m_k [25, 31]. When viewed in this latter form, the model falls in the broad class considered by Harris and Touchette [20, 21]. The results presented here are consistent with the general theoretical arguments of [20, 21].

The large- k behaviour of this model depends on the value of J . For large k , the magnetisation m_k converges to a limiting value. It is convenient to refer to this as a steady state for the model, even though the cluster is constantly growing so the system is not stationary. Given some m_k , the conditional average of s_{k+1} is $\langle s_{k+1} \rangle_{m_k} = \tanh Jm_k$. For large k one finds

$$\langle m_{k+1} \rangle_{m_k} \simeq m_k + \frac{\tanh(Jm_k) - m_k}{k}. \quad (5)$$

This means that steady state values of the magnetisation must solve $m = \tanh Jm$ [22]. This equation is familiar from mean-field models of ferromagnets: there is only one solution if $J \leq 1$ but for $J > 1$ there are three solutions. In this case, the steady states have $m = \pm m_S$ where m_S is the spontaneous magnetisation. The point $m = 0$ is an unstable fixed point of (5) and is not a steady state of the growth model.

We consider trajectories with a total of K steps, and we discuss an LDP that applies for large K . The analogue of the time-average in (1) is m_K , as defined in (3). The LDP discussed by KGGW is similar to (2): as $K \rightarrow \infty$ one has

$$p(m_K) \simeq \exp[-KI(m_K)] \quad (6)$$

where I is the rate function. This is an LDP with speed K [1, 18]. We assume that I is continuous, which is consistent with our results and those of KGGW. Define

$$\mathcal{I}_K(m, \epsilon) = -\frac{1}{K} \log \text{Prob}(|m_K - m| \leq \epsilon). \quad (7)$$

where $\text{Prob}(\dots)$ on the right hand side denotes the probability that m_K is within ϵ of some value m . From the theory of LDPs [1], one has

$$\lim_{K \rightarrow \infty} \mathcal{I}_K(m, \epsilon) = \inf_{x \in [m-\epsilon, m+\epsilon]} I(x). \quad (8)$$

Hence, analysis of \mathcal{I} provides information about the rate function. In particular, the assumed continuity of I means that $I(m) = \lim_{\epsilon \rightarrow 0} \lim_{K \rightarrow \infty} \mathcal{I}_K(m, \epsilon)$.

B. Approximate Langevin equation for m

For large k , the increment in m_k on a single step is small. In this situation, the behaviour of the magnetisation can be described by a Langevin equation. One promotes the step k to a continuous variable and considers the first and second moments of $m_k - m_{k-1}$, for large k . This suggests that we approximate the dynamics of m as

$$k \frac{dm}{dk} = \tanh Jm - m + \frac{1}{\cosh Jm} \eta \quad (9)$$

which is to be interpreted in Ito calculus. Here η is a Gaussian white noise with mean zero and $\langle \eta(k) \eta(k') \rangle = \delta(k - k')$. Note that the Gaussian approximation for the noise does not capture the fact that the growth model always has $|m| \leq 1$. Bearing this in mind, it is convenient to make an additional approximation and replace the multiplicative noise by a simple additive one. This does not change any qualitative aspects of the behaviour and simplifies the analysis. The result is

$$k \frac{dm}{dk} = \tanh Jm - m + \eta \quad (10)$$

It is useful to change variables to $u = \log k$. This yields

$$\frac{dm}{du} = \tanh Jm - m + e^{-u/2} \xi \quad (11)$$

where ξ is a new Gaussian white noise with $\langle \xi(u) \xi(u') \rangle = \delta(u - u')$. (The prefactor of $e^{-u/2}$ appears because rescaling the time co-ordinate in Langevin equations requires a rescaling of the noise variance, to ensure that the random increment on any time-interval is preserved.)

From (11), the natural time scale for the deterministic evolution of m is $u = \log k$. For large values of u , the noise strength is strongly suppressed, leading to almost-deterministic behaviour. The results presented here use the original discrete-time growth model, but all qualitative features can be reproduced in the Langevin model too.

C. Reversible model of growth

The reversible model considered by KGGW was introduced in [22]. It is similar to the irreversible one, except that particles may leave the cluster as well as being added to it. (Note however, this is not a reversible Markov chain in the mathematical sense.) The number of particles in the cluster after step k is N_k and its (extensive) magnetisation is M_k . Also $m_k = M_k/N_k$ is the intensive magnetisation. There are several LDPs that could be considered, including the joint probability distribution for M_K/K and N_K/K , which was analysed by KGGW [11]. Here we consider the behaviour of m_k , for which we expect that

$$p(m_K) \simeq \exp[-KI(m_K)]. \quad (12)$$

This is analogous to (6), although the functional form of I will be different.

The dynamical rule for the model may be formulated in terms of increments $\Delta M_k = M_{k+1} - M_k$ and $\Delta N_k = N_{k+1} - N_k$. The physical idea [22] is that particles are added with rates that do not depend on their spin, but their unbinding rate is suppressed if they are aligned with the magnetisation of the cluster. Specifically

$$(\Delta N_k, \Delta M_k) = \begin{cases} (+1, +1), & \text{w/prob } (c/z_k) \\ (+1, -1), & \text{w/prob } (c/z_k) \\ (-1, +1), & \text{w/prob } e^{Jm_k}(1 - m_k)/z_k \\ (-1, -1), & \text{w/prob } e^{-Jm_k}(1 + m_k)/z_k \end{cases} \quad (13)$$

where

$$z_k = 2(c + \cosh Jm_k - m \sinh Jm_k) \quad (14)$$

is a normalisation constant.

The steady states of this model are described in [22]. There are symmetry-breaking transitions, similar to the irreversible model, but with some additional complexity. We give a brief summary of the relevant behaviour in Section IV, which also includes results for this model.

D. Bounds on probabilities via optimal control theory

One method for analysing large deviations is to establish upper bounds on the rate function, by considering processes where the rare events of interest become typical. This idea is common in the mathematical theory of large deviations [1], its application in physics is reviewed in [32], which also discusses its connection with optimal control theory [33]. This connection provides us with a useful terminology: we consider *control forces* which are added to the system, in order to enhance the probability of rare events (for a physical example, see [34]).

In mathematical studies, one usually aims to prove bounds on rate functions. In KGGW [11], bounds were evaluated numerically, by direct simulation of the growth model, see also [25, 26]. (This approach may be contrasted with other numerical methods [34–39], which use control forces to aid the computation of rate functions or other large-deviation properties, instead of computing bounds.)

We outline the derivation of the relevant bound, following [11, 25]. The method is very general, we focus here on the irreversible growth model. Let $p_k(s|m)$ be the probability that the $(k+1)$ th particle has spin s , given that the magnetisation just after step k is m . The probability of a trajectory $\mathbf{m} = (m_1, m_2, \dots, m_K)$ for the original process is $P(\mathbf{m}) = \prod_{k=1}^K p_k(s_k|m_{k-1})$, with $s_k = m_{k+1} - m_k$. In the irreversible model, (4) shows that $p_k(s|m) = [1 + \exp(-2Jms)]^{-1}$, for $k \geq 2$. This is independent of k because the update rule does not depend on

k , except through the value of m_k . The initial condition is specified by taking $p_1(s|m) = (1/2)$ (for $s = \pm 1$).

Now introduce a *controlled system* in which the corresponding transition probabilities are $p_k^{\text{con}}(s_{k+1}|m_k)$. In [11, 25, 26], this process is called the reference system. The average of some observable quantity F in the controlled process is denoted by $\langle F \rangle_{\text{con}}$, and the corresponding average in the original system is $\langle F \rangle$. By considering the probabilities of individual trajectories, one sees that

$$\langle F \rangle = \langle F \exp[-\mathcal{A}(\mathbf{m})] \rangle_{\text{con}} \quad (15)$$

where the action \mathcal{A} is

$$\mathcal{A}(\mathbf{m}) = \sum_{k=1}^K \log \frac{p_k^{\text{con}}(s_k|m_{k-1})}{p_k(s_k|m_{k-1})}. \quad (16)$$

We define an indicator function $\chi_\epsilon(x)$ that is equal to unity if $|x| < \epsilon$, and zero otherwise. Then use (7) to write $\mathcal{I}_K(m, \epsilon) = -K^{-1} \log \langle \chi_\epsilon(m_K - m) \rangle$. Using (15) to express the right hand side in terms of averages with respect to the controlled process, and noting that e^x is convex, one obtains by Jensen's inequality [11, 25] that

$$\mathcal{I}_K(m, \epsilon) \leq \mathcal{H}_K(m, \epsilon) \quad (17)$$

with

$$\mathcal{H}_K(m, \epsilon) = -\frac{1}{K} \log \langle \chi_\epsilon(m_K - m) \rangle_{\text{con}} + \frac{\langle \chi_\epsilon(m_K - m) \cdot \mathcal{A}[\mathbf{m}]/K \rangle_{\text{con}}}{\langle \chi_\epsilon(m_K - m) \rangle_{\text{con}}}. \quad (18)$$

The first term on the right hand side of (18) is the log probability of the event that $|m_K - m| \leq \epsilon$, in the controlled process. The second term is a conditional average of the action, which is obtained by averaging over the trajectories that realise this event. If this event of interest is typical under the controlled dynamics, it is simple to evaluate \mathcal{H} and hence to obtain an upper bound on \mathcal{I} . Obtaining accurate bounds (with $\mathcal{H} \approx \mathcal{I}$) requires a good choice of the controlled process.

For ergodic Markov processes in the classes considered by [7, 24, 29] (which include irreducible finite-state Markov chains and a large class of stochastic differential equations), the search for suitable controlled processes is somewhat simplified. In these cases, it can be shown [17, 24, 29] that for $K \rightarrow \infty$ one may achieve equality in (17) by using a controlled process where the transition probabilities do not depend on the step k (except possibly for $k = 1$, which controls the initial condition). However, the situation for growth models is more complicated because achieving equality in (17) may require a controlled process whose transition rates depend explicitly on k . The new results that we obtain here are obtained by considering this type of controlled process.

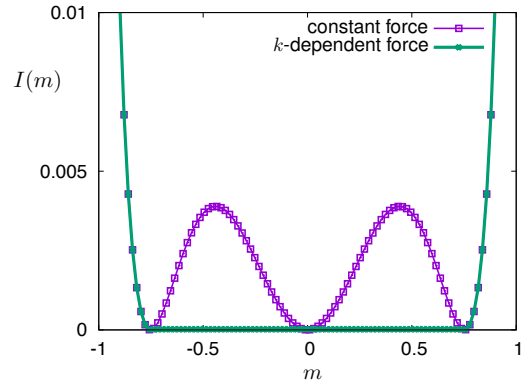


FIG. 1. Upper bounds on the rate function for the LDP (6) in the irreversible model, for the representative case $J = 1.3$. We show the bound of KGGW, which is obtained using control forces that are constant (independent of k). This is compared with our new bound, which uses control forces that depend on k . They differ for $|m| < m_S$ where our new result (with k -dependent forces) implies that $I(m) = 0$.

III. RESULTS : IRREVERSIBLE MODEL

A. LDP with speed K

We first analyse the LDP (6) in the irreversible model. For $J < 1$, the system has a single steady state. In this case, KGGW predicted [11] that the rate function I has a unique zero at $m = 0$, and is convex for all $m \in (-1, 1)$. They show how this rate function can be bounded by using (17) and they explain that this bound should be saturated. This prediction is also consistent with [21].

In this section, we consider systems with $J > 1$. We derive improved bounds on the rate function, for $|m| < m_S$. (Recall that the steady state of the model spontaneously breaks up-down symmetry in this case, and the magnetisation of the steady state is $\pm m_S$.) Fig. 1 summarises the result, which is that $I(m) = 0$ for $|m| \leq m_S$. Outside this range, we obtain the same results as KGGW.

It is notable that for many LDPs, zeros of the rate function $I(m)$ correspond to typical values of the observable m [18]. The situation shown in Fig. 1 is different, in that the typical values of m are $\pm m_S$ but the rate function is zero throughout the range $|m| \leq m_S$. This behaviour occurs when the probability density for m decays to zero less fast than an exponential [for example $p(m_K) \sim K^{-\alpha}$ so that $p(m_K) \rightarrow 0$ at large K , but one still has $\mathcal{I}_K(m, \epsilon) \rightarrow 0$, and hence $I(m) = 0$ by (8)]. This behaviour may be somewhat unusual but it is fully consistent with the existence of a large deviation principle with speed K [1]. It is also similar to the behaviour of the free energy in thermodynamic systems close to phase coexistence, see Sec. V.

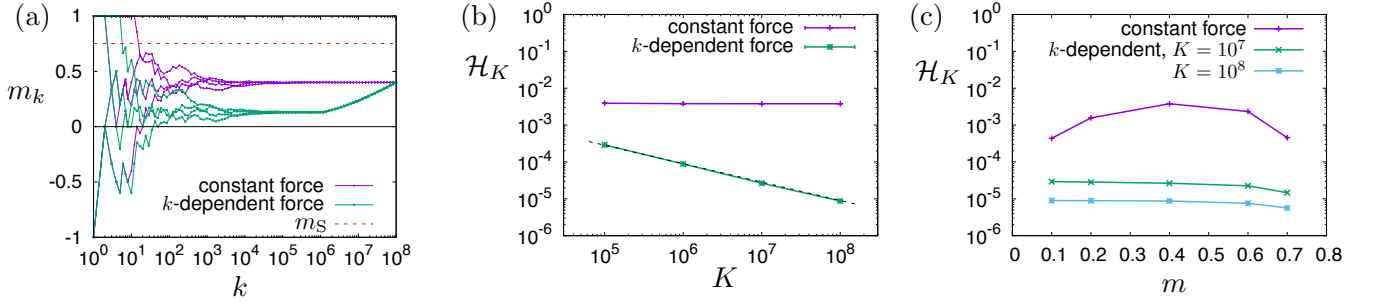


FIG. 2. Results for the irreversible growth model in the representative case $J = 1.3$, for which $m_S \approx 0.75$. (a) Trajectories of the controlled dynamics for $K = 10^8$, which all achieve $m_K \approx 0.4$. For the k -dependent force then $(b, k^*) = (0.13, 1.2 \times 10^6)$. (b) Results for \mathcal{H}_K using the same controlled dynamics, as a function of K . (For the time-dependent forces, the values of b, k^* are different for each K .) Error bars are comparable with symbol sizes. The dashed line is the prediction of (27), without any fitting parameters. (c) The behaviour of \mathcal{H}_K as a function of m . The data in (b,c) and the agreement with (27) indicate that $\lim_{K \rightarrow \infty} \mathcal{H}_K(m, \epsilon) = 0$ throughout the range $|m| < m_S - \epsilon$, so $\lim_{K \rightarrow \infty} \mathcal{I}_K(m, \epsilon) = 0$ within this range, by (17).

1. Control forces that are independent of k

We first derive the bounds of KGGW, following their method, which uses (17). We use a slightly different controlled system in which the extensive magnetisation $M_k = km_k$ follows a biased random walk (see also [25, 31]). The dynamical rule for this controlled system is

$$s_{k+1} = \begin{cases} +1, & \text{with prob } (1+b)/2 \\ -1, & \text{with prob } (1-b)/2 \end{cases} \quad (19)$$

where b is a numerical parameter with $|b| \leq 1$. In this case, the mean and variance of m_k under the controlled dynamics are

$$\langle m_k \rangle_{\text{con}} = b, \quad \langle (\Delta m_k)^2 \rangle_{\text{con}} = (1 - b^2)/k. \quad (20)$$

For large k , the variance tends to zero and m_k becomes sharply peaked at b . This allows calculation of \mathcal{H}_K in (18), and hence bounds on \mathcal{I}_K . For large K then $\langle \chi_\epsilon(m_K - b) \rangle_{\text{con}} \rightarrow 1$. Also, from (19) one has $p_K^{\text{con}}(s|m) = (1 + sb)/2$, independent of m , so (18) yields

$$\langle \mathcal{A}(m)/K \rangle_{\text{con}} \simeq \frac{1+b}{2} \log \frac{(1+b)(1+e^{-2Jb})}{2} + \frac{1-b}{2} \log \frac{(1-b)(1+e^{2Jb})}{2} \quad (21)$$

We used that the fraction of steps with $s_k = \pm 1$ is $(1 \pm b)/2$ and the contribution to the action for each such hop is $\log[(1 \pm b)(1 + e^{\mp 2Jm})/2]$; also m_k is sharply peaked at b , so the *average* action for such a hop can be estimated as $\log[(1 \pm b)(1 + e^{\mp 2Jb})/2]$. Since m_k is sharply peaked, we note that this result for the action is somewhat insensitive to details of the controlled dynamics. For example, if the rates in (19) depended on also m_k , the action would only be sensitive to the values of the rates at the mean value of m_k . This insight is related to the temporal additivity principle of Harris and Touchette [20, 21]. In our context,

it means that adding extra complexity to the controlled process (19) does not yield improved bounds on \mathcal{I} .

Using again that m_K is sharply peaked, the conditional average of the action in (18) can be replaced by the simple average in (21), and one obtains (after simplifying the right hand side of (21) and setting $b = m$)

$$\mathcal{H}_K(m, \epsilon) \simeq \frac{1}{2} \log(1 - m^2) + \log \cosh(Jm) + \frac{m}{2} \log \frac{1+m}{1-m} - Jm^2 \quad (22)$$

as in [11]. This result is valid for large K . It is easily checked that $\mathcal{H}_K(m, \epsilon)$ is non-negative for all m (as it must be, since it is a bound on \mathcal{I}). Using $2 \tanh^{-1} m = \log(1+m)/(1-m)$, one also sees that $\mathcal{H}_K(m, \epsilon) = 0$ if $m = \tanh(Jm)$. That means that $\mathcal{I}_K(m, \epsilon) = 0$ if m is fixed point of (5). For $b \ll 1$ we also obtain

$$\langle \mathcal{A}(m)/K \rangle_{\text{con}} \simeq \frac{b^2(J-1)^2}{2} + \mathcal{O}(b^4) \quad (23)$$

which determines the action of trajectories that are close to the $m = 0$ (unstable) fixed point.

At this fixed point, one sees that $\mathcal{I}_K(m, \epsilon) \simeq 0$ (for large K). This means that trajectories with $m_K = 0$ have probabilities that do not decay exponentially in K . The physical interpretation of this fact is that if the growing cluster contains a symmetric mixture of up and down spins, there is no force that acts to increase or decrease the magnetisation. On the other hand, if m is intermediate between 0 and m_S , there is a force that drives the system towards the stable fixed point at m_S . This is the intuition behind the LDP (6): the probability to remain for a long time at a non-typical value of m is suppressed exponentially in K , because of the forces in the model that tend to drive m towards a typical value. At $m = 0$, the force is zero, so the probability to remain near this value is suppressed less strongly.

So far, all results are fully consistent with KGGW [11]. We now show that for $m < m_S$, the true value of \mathcal{I}_K is

much less than \mathcal{H}_K in (22). We will obtain improved bounds by taking a controlled process in (17) in which the transition rates depend explicitly on the step k .

2. Control forces that depend on k

We take a controlled process that is a mixture of (19) and (4), as follows. We choose two parameters, which are the bias b in (19) and a step k^* at which the controlled dynamics changes its character. For the early part of the trajectory, which is $k \leq k^*$, the controlled system is an asymmetric random walk as in (19); for the later part ($k > k^*$) we revert to the original dynamics (4). One sees that the action \mathcal{A} in (16) has no contribution from the later part of the path. Since smaller values of \mathcal{A} lead to more accurate bounds, this is a desirable feature. We restrict to $|b| < m_S$ which is sufficient for our purposes.

Typical trajectories of this controlled dynamics are illustrated in Fig. 2(a). If $b^2 k^* \gg 1$ then one sees from (20) that the distribution of m_{k^*} is sharply peaked, in the sense that its mean b is much larger than its standard deviation, which is of order $(k^*)^{-1/2}$. In this case, the distribution of m_k also remains sharply peaked for the later part of the trajectory. For $k > k^*$, the system follows the original dynamics and the mean of m_k can be obtained from (5) by solving $dm/dk = (\tanh Jm - m)/k$, as in [11]. As in (11), is natural to change variables to $u = \log k$ so that

$$\frac{dm}{du} = \tanh Jm - m. \quad (24)$$

This means that for $k > k^*$, trajectories will flow away from the unstable fixed point at $m = 0$ and towards the stable point at $m = m_S$, as in Fig. 2(a). Moreover, this evolution is very slow: the natural time variable is not the number of steps k but the rescaled “time” $u = \log k$. (Physically, the slow variation with k occurs because there are already many particles in the cluster, so making a significant change in its magnetisation requires the addition of many particles.)

In order to establish a bound on $\mathcal{I}_K(m, \epsilon)$, we treat m as a target value for m_K : suitable controlled processes should hit this target with high probability. We choose b and k^* to achieve this, as follows.

We solve (numerically) the differential equation (24), going backwards in time. This yields a path which ends at $m_K = m$ and can be propagated back to any earlier time k , for example by Euler’s method. The magnetisation on this path is $\tilde{b}(k)$ with $k \leq K$ and $\tilde{b}(K) = m$. Both k and $\tilde{b}(k)$ decrease as we solve the equation backwards in time. As $k \rightarrow 0$ then $\tilde{b} \rightarrow 0$. (Note that $m = 0$ is an unstable fixed point of the forward equation, which corresponds to a stable fixed point of the backward equation.) We stop the solution at the point $(k, \tilde{b}) = (k^*, b)$ where

$$b^2 k^* = a\sqrt{K} \quad (25)$$

where a is a numerical parameter, of order unity (we take $a = 2$, results depend weakly on this choice).

These b, k^* are the parameters that we use for the controlled dynamics. As long as K is reasonably large, the algorithm gives $b \ll 1$ and $k^* \gg 1$. Then the action for this controlled process can be estimated from (23), with K replaced by k^* . This yields

$$\langle \mathcal{A} \rangle_{\text{con}} \approx k^* \frac{b^2 (J-1)^2}{2}. \quad (26)$$

Since (b, k^*) solve (25), this means that $\langle \mathcal{A} \rangle_{\text{con}}$ is of order \sqrt{K} . Combining this result with (18) and assuming that the controlled system hits the target with probability 1, one obtains

$$\mathcal{H}_K(m, \epsilon) \simeq \frac{a(J-1)^2}{2\sqrt{K}}. \quad (27)$$

Hence, the bound \mathcal{H}_K tends to zero as $K \rightarrow \infty$. This result applies for large K and is independent of the target chosen for m_K (always assuming that this target is between ϵ and $m_S - \epsilon$). Note however, that the controlled process depends on K , in that the parameters b, k^* are chosen separately for each value of K . The assumption that the controlled system hits the target with probability 1 is valid as long as the magnetisation distribution at k^* is sharply-peaked in the sense that its mean is much larger than its standard deviation. This requires $b^2 k^* \gg 1$ which is true by (25) as long as K is large.

Numerical results based on this construction are shown in Fig. 2. In particular, Fig. 2(a) shows that the parameters (b, k^*) obtained by this method are such that the controlled system hits the target m with high probability. Also, Fig. 2(b) confirms that on increasing K , the bound \mathcal{H}_K is quantitatively consistent with (27). This establishes that $\lim_{K \rightarrow \infty} \mathcal{H}_K(m, \epsilon) = 0$, and hence from (17) one has $\lim_{K \rightarrow \infty} \mathcal{I}_K(m, \epsilon) = 0$, for this value of m . Fig. 2(c) shows that the same behaviour occurs for several values of m with $|m| < m_S - \epsilon$. This is expected since the theoretical argument above is independent of the target for m_K . Hence $\lim_{K \rightarrow \infty} \mathcal{I}_K(m, \epsilon) = 0$ throughout this range, which establishes that the rate function (6) obeys

$$I(m) = 0, \quad |m| < m_S. \quad (28)$$

That is, the rate function in (6) is positive and convex for $|m| > m_S$ and is equal to zero for all $|m| \leq m_S$. This was the result anticipated in Fig. 1. We emphasise that while the numerical results in Fig. 2 are a useful confirmation of our theoretical calculations, the bound in (27) is an analytical result.

B. Scaling of $\text{Prob}(|m_K - m| < \epsilon)$

As $K \rightarrow \infty$, we have shown that $\mathcal{I}_K(m, \epsilon) \rightarrow 0$ throughout the regime $|m| \leq m_S - \epsilon$. This shows that $\text{Prob}(|m_K - m| < \epsilon)$ does not decay exponentially with K . Nevertheless, we expect that this probability should

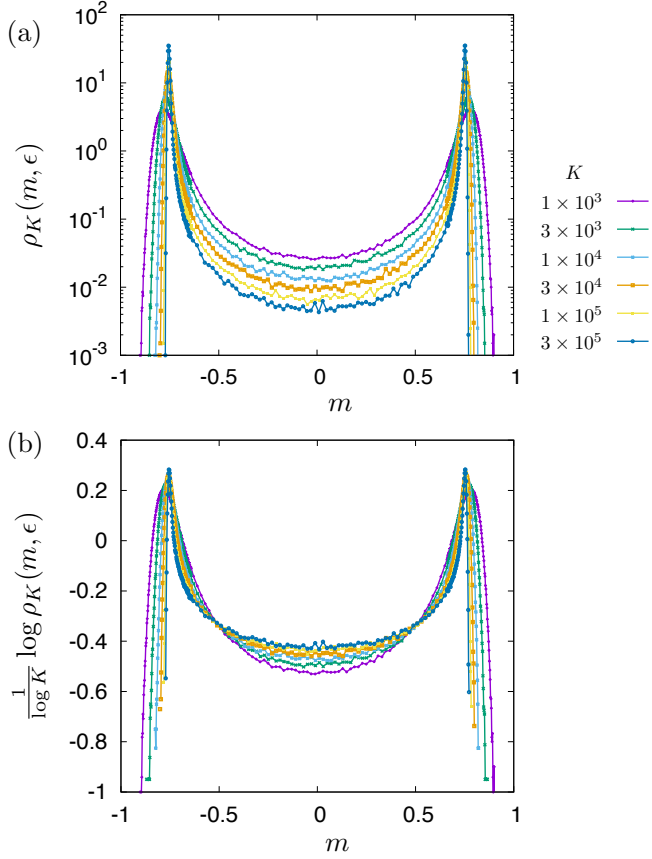


FIG. 3. (a) Estimated probability density for m_K obtained by direct sampling of the irreversible growth model at $J = 1.3$. Note that K varies over more than two decades. The binning parameter is $\epsilon = 10^{-3}$ for values of m near the peaks and $\epsilon = 10^{-2}$ for intermediate values. (Results depend weakly on ϵ , which is chosen to reduce statistical uncertainties while maintaining adequate resolution.) (b) The logarithms of the same probability densities, scaled by $\log K$. The prediction (31) is that for every $|m| < m_S$ one should observe convergence of this quantity to some negative (non-zero) limit, as $K \rightarrow \infty$. The data are consistent with this prediction.

vanish as $K \rightarrow \infty$, so the natural question is: how small is it?

To address this question we define an estimate of the probability density for m_K as

$$\rho_K(m, \epsilon) = \frac{1}{2\epsilon} \text{Prob}(|m_K - m| \leq \epsilon) \quad (29)$$

(In the previous section we preferred to analyse probabilities instead of densities, in order to avoid issues with divergence of the probability density for sharply-peaked distributions. For this section, we work with ρ_K but we emphasise that ϵ is to be kept finite as $K \rightarrow \infty$.)

Fig. 3(a) shows the distribution of m_K , obtained by direct sampling of trajectories of the system, for the representative parameter value $J = 1.3$. Two features are notable. First, the probability that $m_K \approx 0$ is small and decreases with K , but the decay is much slower

than exponential in K , consistent with the arguments of section III A. Second, there is no evidence for a local maximum in the probability at the unstable fixed point $m_K = 0$. The parameter $J = 1.3$ is representative of the regime with $J > 1$, in particular we have verified that similar results are also obtained for larger J .

We note in passing that the the distribution of m_K shows two sharp peaks in Fig. 3 and the width of each peak scales as $K^{-1/2}$ (this follows from the arguments about sharply-peaked distributions given above, it is also consistent with the existence of a central limit theorem for $|m_K|$, see [22]). In the picture of Fig. 1, the variance of $|m_K|$ may be obtained from the second derivative of the rate function as $I''(m_S^+)^{-1}$, where the notation m_S^+ indicates that one should evaluate the second derivative I'' via a limit where m tends to m_S from above. (This is consistent with the usual interpretation that the value of $I''(m)$ at a typical value of m is related to the width of the peak in the probability density [18]. The subtlety in this model is that I'' is discontinuous at $\pm m_S$, so it is necessary to specify how the derivative should be evaluated.)

To estimate ρ_K for $|m| < m_S$, it is possible to repeat the argument of Sec. III A replacing (25) with $b^2 k^* = aK^\alpha$ for some $\alpha \in (0, 1)$. This can be used to show that for any $\beta > 0$ one has

$$\lim_{K \rightarrow \infty} K^{-\beta} \log \text{Prob}(|m_K - m| < \epsilon) = 0, \quad (30)$$

for $|m| \leq (m_S - \epsilon)$ as usual. In other words, the probability of a non-typical value of m_K decays slower than $\exp(-cK^\beta)$, for any c, β . Based on this observation, we propose that the probability decays as a power law in K . In that case

$$\mathcal{J}_K(m, \epsilon) = -\frac{\log \rho_K(m, \epsilon)}{\log K} \quad (31)$$

should have a positive (non-zero) limit as $K \rightarrow \infty$. Fig. 3(b) shows results that are consistent with (31). We now present theoretical arguments that further support this conjecture, including bounds based on (17).

1. Accurate bounds for large K

Consider the same controlled dynamics as in Sec. III A, but with $b = 0$. The remaining parameter is k^* : this means that the extensive magnetisation M_k in the controlled process is a simple (unbiased) random walk for $k < k^*$. We use the original growth dynamics (4) for $k > k^*$. In this case the distribution of m_{k^*} has mean zero and its standard deviation is $(k^*)^{-1/2}$, by (20). We will take $k^* \gg 1$ so the distribution of m_{k^*} is sharply-peaked in the sense that its variance is small compared to unity. However, in contrast to Sec. III A, this distribution does not remain sharply-peaked under the time evolution (see below).

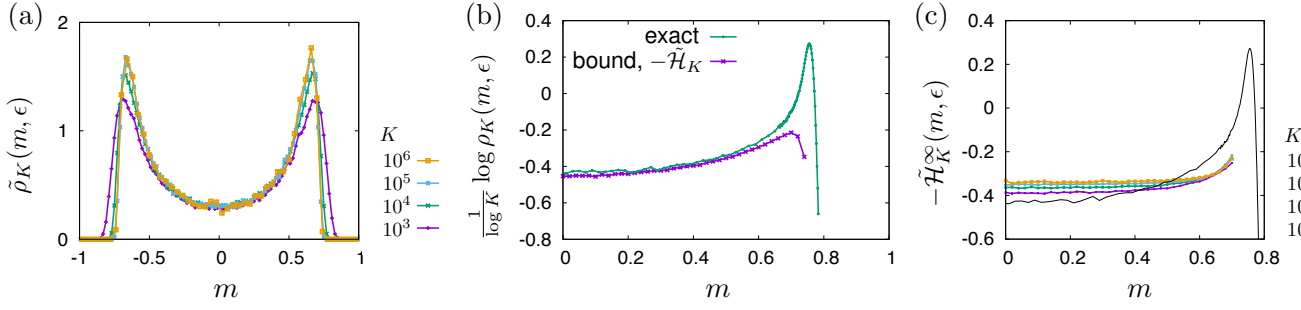


FIG. 4. Irreversible model with $J = 1.3$. (a) Probability distribution of m_K under the controlled dynamics, with k^* chosen as in (32). The form of the distribution depends weakly on K and the probability density is of order unity across a wide range of m . (b) The bound (34) for $K = 10^5$, compared with the (numerically) exact distribution ρ_K for the original model, obtained by direct sampling. (c) The negative of the asymptotic bound $\tilde{\mathcal{H}}_K^\infty$ that appears in (36), for various K . As an illustrative comparison, this is compared with the (numerically) exact distribution at $K = 10^5$ from panel (b), shown as a thin black line. We emphasise that the asymptotic bound is not a bound on this finite- K distribution

To fix a suitable value for k^* , it is useful to consider the deterministic evolution of the mean of m_k for $k > k^*$, assuming that m_{k^*} has a typical value of order $(k^*)^{-1/2}$. Since m is small, one may linearise (24), leading to $(dm/du) = (J - 1)m$ and hence $m_k = m_{k^*}(k/k^*)^{J-1}$. We choose k^* in such a way that this deterministic equation gives $m_K = O(1)$. This leads to

$$k^* = \gamma K^{\frac{J-1}{J-(1/2)}} \quad (32)$$

with γ a constant of order unity. We take $\gamma = 1$.

By analogy with (29), we define an estimate of the probability density for m_K under the controlled dynamics as

$$\tilde{\rho}_K(m, \epsilon) = \frac{1}{2\epsilon} \text{Prob}_{\text{con}}(|m_K - m| \leq \epsilon) \quad (33)$$

where Prob_{con} indicates a probability under the controlled dynamics. Numerical results for $\tilde{\rho}$ are shown in Fig. 4(a), for several values of K , always with k^* chosen according to (32). One sees that the distributions of m_K are not sharply peaked. Instead $\tilde{\rho}$ is of order unity everywhere between $\pm m_S$. Moreover, this distribution depends very weakly on K (which varies over three decades). This is due to the choice proposed in (32): the value of γ is not important but the correct power-law exponent is essential. (Different values of γ lead to different distributions, but they are all similarly broad.)

Repeating the argument of Sec. IID, one obtains

$$\mathcal{J}_K(m, \epsilon) \leq \tilde{\mathcal{H}}_K(m, \epsilon) \quad (34)$$

with

$$\begin{aligned} \tilde{\mathcal{H}}_K(\rho, \epsilon) &= \frac{-1}{\log K} \log \tilde{\rho}_K(m, \epsilon) \\ &+ \frac{1}{\log K} \frac{\langle \chi_\epsilon(m_K - m) \mathcal{A}[\mathbf{m}] \rangle_{\text{con}}}{\langle \chi_\epsilon(m_K - m) \rangle_{\text{con}}}. \end{aligned} \quad (35)$$

This bound is shown in Fig. 4(b), for the representative case $K = 10^5$. It shows almost quantitative agreement

over a range of m that includes $m = 0$. However, the agreement breaks down as m gets close to m_S . (Better bounds for larger m might be obtained by using smaller c in (32), but we have not explored this in detail.)

2. Asymptotic behaviour as $(\log K) \rightarrow \infty$

The numerical bound in Fig. 4(b) is valid at $K = 10^5$ and gives a reasonable estimate of the probability density, but the regime of primary interest is $K \rightarrow \infty$. Based on Fig. 4(a), we expect that $\log \tilde{\rho}_K(m, \epsilon)$ remains of order unity as $K \rightarrow \infty$. In this case, its contribution to $\tilde{\mathcal{H}}_K$ will decay proportional to $1/(\log K)$ and the term involving \mathcal{A} will dominate (35) at large K . It is useful to estimate this term directly, in order to predict the behaviour of \mathcal{H}_K as $K \rightarrow \infty$. That is, assuming that $\log \tilde{\rho}$ remains finite as $K \rightarrow \infty$, one has from (34,35) that

$$\lim_{K \rightarrow \infty} \mathcal{J}_K(m, \epsilon) \leq \lim_{K \rightarrow \infty} \tilde{\mathcal{H}}_K^\infty(m, \epsilon) \quad (36)$$

with

$$\tilde{\mathcal{H}}_K^\infty(m, \epsilon) = \frac{1}{\log K} \frac{\langle \chi_\epsilon(m_K - m) \mathcal{A}[\mathbf{m}] \rangle_{\text{con}}}{\langle \chi_\epsilon(m_K - m) \rangle_{\text{con}}}. \quad (37)$$

We refer to this as an asymptotic bound since it does not bound \mathcal{J}_K at any finite K , but only as $K \rightarrow \infty$: see (36). For finite K , the difference between the exact bound and the asymptotic bound scales as $(1/\log K)$, which decays very slowly with K . This means that the asymptotic behaviour is not easily accessible in numerics. However, the asymptotic bound can be evaluated numerically for finite K and provides an estimate of the right hand side of (36).

Results are shown in Fig. 4(c). The estimates for the asymptotic bound are compared with the actual distribution for $K = 10^5$. One sees that the asymptotic bound in Fig. 4(c) depends weakly on m , over a fairly wide range that includes $m = 0$. This bound is evaluated numerically as an average of \mathcal{A} , which is restricted to trajectories

whose final magnetisation m_K is within the relevant bin of a suitably constructed histogram. We do not have a theoretical estimate of this conditional average. However, the unconditioned average of the action can be obtained from (16) as

$$\langle \mathcal{A}(\mathbf{m}) \rangle_{\text{con}} \simeq \sum_{k=1}^{k^*} \left\langle \frac{1}{2} \log \frac{(1 + e^{-2Jm_k})(1 + e^{2Jm_k})}{4} \right\rangle_{\text{con}} \quad (38)$$

For $1 \ll k \ll k^*$ then m_k is small under the controlled dynamics and its variance is $1/k$. Hence, we expand (38) to second order in m_k , which yields $\langle \mathcal{A}(\mathbf{m}) \rangle_{\text{con}} \approx \sum_k J^2/(2k)$. Approximating the sum by an integral leads to

$$\langle \mathcal{A}(\mathbf{m}) \rangle_{\text{con}} \simeq \frac{J^2}{2} \log k^* + A_0. \quad (39)$$

where A_0 is a constant of order unity which depends on the behaviour of trajectories when k is of order unity. (The behaviour of the system for $k = O(1)$ is not captured by our various approximations so we are not able to estimate this constant analytically.)

If we now assume that the conditional average of the action in (18) is the same as the corresponding unconditioned average then (32,35,39) together yield

$$\tilde{H}_K^\infty(m, \epsilon) \simeq \frac{J^2(J-1)}{2J-1}. \quad (40)$$

which is independent of m . Using the unconditioned average as an estimate of the conditioned one is an uncontrolled approximation, but (40) is consistent with the weak dependence of \tilde{H}_K^∞ on m in Fig. 5c. For that case, (40) evaluates to 0.32, consistent with the data for small and moderate m (given that we are still far from the limit where $\log K$ is large).

Based on this analysis, we summarise our conclusions for the probability distribution of m_K , at large K . We have argued that for $|m| < (m_S - \epsilon)$ then $\mathcal{J}_K(m, \epsilon)$ has a finite limit as $K \rightarrow \infty$, which means that $\rho_K(m, \epsilon)$ decays as a power law. Based on the asymptotic bound in Fig. 4c, we offer two possibilities for the detailed behaviour of \mathcal{J}_K . The first is that $\lim_{K \rightarrow \infty} \mathcal{J}_K(m, \epsilon)$ is independent of m within some range including zero, and that it takes a value α within that range. From (40), we expect $\alpha \approx J^2(J-1)/(2J-1)$ in this case. The result would be that

$$\rho_K(m, \epsilon) \simeq t^{-\alpha} f(m, \epsilon) \quad (41)$$

within the relevant range of m , with $f(m, \epsilon)$ of order unity. The extreme version of this scenario would be that the relevant range is $|m| < m_S - \epsilon$: this is not apparent from the finite- K data presented here but we are still far from the limit where $\log K \rightarrow \infty$. In any case this limit is not expected to commute with a limit where $m \rightarrow (m_S - \epsilon)$ so one may expect significant deviations from the asymptotic (large- K) behaviour in

data obtained at finite K . The second scenario is that $\lim_{K \rightarrow \infty} \mathcal{J}_K(m, \epsilon) = \alpha(m, \epsilon)$ where α is now a function which takes values of order unity. In this case

$$\rho_K(m, \epsilon) \simeq t^{-\alpha(m, \epsilon)}. \quad (42)$$

This might be interpreted as a large deviation principle with speed $(\log t)$, because the distribution of m_K scales as $p(m_K) \sim e^{-(\log t)\beta(m_K)}$, where β would be interpreted as a rate function [with $\beta(m) = \lim_{\epsilon \rightarrow 0} \alpha(m, \epsilon)$]. However, establishing such an LDP would require a detailed mathematical analysis that is beyond the scope of this work.

Based on the available numerical data, we are not able to settle which (if either) of (41,42) is valid, because all results are limited by the fact that the numerical parameter $\log K$ governs the convergence to the large- K regime, and this number is never very large. To address this, we suggest that the Langevin equation (11) might be tractable in the regime where $u = \log k$ is very large, but this analysis is beyond the scope of this work.

IV. RESULTS : REVERSIBLE MODEL

In this section we analyse large deviations in the reversible model of growth, which was defined in Sec. II C. This demonstrates that the use of time-dependent control forces to obtain improved bounds can be generalised beyond the single system considered so far. We focus on a representative state point where the deterministic dynamics has an unstable fixed point at non-zero magnetisation. This is the case where the model has three steady states. (For parameters where the model has one steady state or two steady states, the behaviour is very similar to that of the irreversible model, so we do not discuss it in detail.)

A. Summary of behaviour and definition of controlled dynamics

We summarise the behaviour of the model, as derived in [22]. We assume throughout that the parameter c in (13) is large enough that the steady state of the system involves a cluster that grows with a constant rate. (The alternative is that there is a steady state with a cluster of finite size, the behaviour is quite different in that case and we do not discuss it here.) For the reversible model, the analogue of (5) is

$$\langle \Delta m_k \rangle_{m_k, N_k} = \frac{(1 - m_k^2) \sinh(Jm_k) - cm_k}{N_k [c + \cosh(Jm_k) - m_k \sinh(Jm_k)]}. \quad (43)$$

where the average is conditioned on the values of m_k and N_k . As noted in [22], this means that steady state values for m solve

$$cm = (1 - m^2) \sinh Jm. \quad (44)$$

For $J > c$ there are three solutions to this equation, and the behaviour is similar to the irreversible model for $J > 1$. For $J < c$ there are two possibilities – either a single solution, or five solutions. The first case corresponds to a single steady state with $m = 0$. The latter case means that there are three possible steady states, which have magnetisations $0, \pm m_S$. In this case there are also two unstable fixed points of (43) at $\pm m_U$ (these are not steady states of the stochastic model, similar to the irreversible case). The situation with three steady states is only possible for $\sqrt{6} < J < c$ (this condition is necessary but not sufficient).

As a suitable controlled dynamics, we take

$$(\Delta N_k, \Delta M_k) = \begin{cases} (+1, +1), & \text{w/prob } (c'/z'_k) \\ (+1, -1), & \text{w/prob } (c'/z'_k) \\ (-1, +1), & \text{w/prob } (1+\lambda)(1-m_k)/z'_k \\ (-1, -1), & \text{w/prob } (1-\lambda)(1+m_k)/z'_k \end{cases} \quad (45)$$

with two parameters λ, c' , also $z'_k = 2(c' + 1 - \lambda m_k)$ for normalisation. This controlled process is similar to that considered in [11], but not identical. In principle one may take different rates for the two cases with $\Delta N_k = +1$, which will lead to improved bounds in some cases. However, (45) is sufficient for our purpose, which is to show that $I(m) = 0$ for $|m| \leq m_S$.

In the steady state of this model, the rate of cluster growth is denoted by r and the magnetisation is denoted by b (by analogy with (20)). Considering the mean increments for N_k and M_k , the rate of cluster growth can be verified to be $r = (c' - 1 + \lambda b)/(c' + 1 - \lambda b)$, which is assumed to be positive, as noted above. Also, b is a solution of $\lambda(b^2 - 1) + bc' = 0$, specifically

$$b = \frac{1}{2\lambda} \left(\sqrt{c'^2 + 4\lambda^2} - c' \right). \quad (46)$$

If $\lambda = 0$ (equal probabilities for unbinding of up and down spins) then $b = 0$ (no magnetisation in steady state).

Using that the cluster size and the magnetisation are both sharply peaked in the steady state, the analogue of (21) may be expressed as

$$\begin{aligned} \langle \mathcal{A}(\mathbf{m})/K \rangle_{\text{con}} &\simeq \log(z/z'_b) + (2c'/z'_b) \log(c'/c) \\ &+ \frac{1-b\lambda}{z'_b} \log(1-\lambda^2) \\ &+ \frac{\lambda-b}{z'_b} \left[\log \frac{1+\lambda}{1-\lambda} - 2Jb \right] \end{aligned} \quad (47)$$

with $z'_b = 2(c' + 1 - \lambda b)$. We emphasise that this formula is valid only if b, c', λ are related by (46), so that b is the magnetisation of the steady state of the controlled process. If $m = b$ is a solution of (44) then one may take $\lambda = \tanh Jb$ and $c' = c/(\cosh Jb)$, and the action evaluates to zero. That is, the action is zero at fixed points of the deterministic growth dynamics (similar to the irreversible case).

B. Bounds on $\mathcal{I}_K(m, \epsilon)$

The main result of this section is that $\mathcal{I}_K(m, \epsilon) \rightarrow 0$ for $|m| < m_S$ and $K \rightarrow \infty$, and hence that the rate function $I(m)$ in (12) is zero throughout this range. This is illustrated in Fig. 5(a), which is similar to Fig. 1. As in the irreversible case, we prove this by obtaining bounds on \mathcal{I}_K .

As in Sec. III A 1, we first consider controlled processes with constant rates (independent of k). This will recover results similar to KGGW. We use (47) with (17) to derive bounds on $\mathcal{I}_K(m, \epsilon)$, for $m = b$. Using

$$c' = \lambda(1 - b^2)/b \quad (48)$$

from above and also substituting for z'_b , the formula (47) for the action may be expressed as a function of (b, λ) . Minimising this function (numerically) over λ , one obtains a bound on \mathcal{I}_K , which is plotted with squares in Fig 5(a). As noted above, the resulting bound is zero for fixed points of the deterministic dynamics (including the unstable fixed points). It is positive for other values of m .

If the growth process has multiple stable states, this bound (obtained with control forces independent of time) does not provide an accurate estimate of \mathcal{I}_K . The reason is similar to the irreversible model. To derive improved bounds we use the fact that the average action is very small if b is close to m_U . We then follow the method that was illustrated in Fig. 2. We introduce the additional parameter k^* and we construct trajectories that have magnetisation b for $k < k^*$, but then follow the natural dynamics of the model for $k > k^*$. The parameters b, k^* are chosen such that the final magnetisation m_K is close to its target value m . The action can then be minimised by taking b close to m_U and k^*/K to be small.

Compared to the irreversible model, the method for choosing b, k^* is different; one must also fix λ , which determines c' via (48). Define $n_k = N_k/k$. Following [22], we derive analogues of (24), which are differential equations for the mean of n_k and m_k as a function of $u = \log k$. These are

$$\frac{dm}{du} = \frac{(1-m^2) \sinh Jm - cm}{n[c + \cosh Jm - m \sinh Jm]} \quad (49)$$

and

$$\frac{dn}{du} = -n + \frac{c - \cosh Jm + m \sinh Jm}{c + \cosh Jm - m \sinh Jm}. \quad (50)$$

These equations will be solved forwards in time, in contrast to the irreversible model. (The reason is that m prescribes a target for m_K but there is no target for n_K , so there are not enough boundary conditions to solve backwards in time.)

Suppose that we are given some K and some target m for m_K . We propose an initial guess for b that is between m_U and m . For this b , we minimise (47) over λ as above,

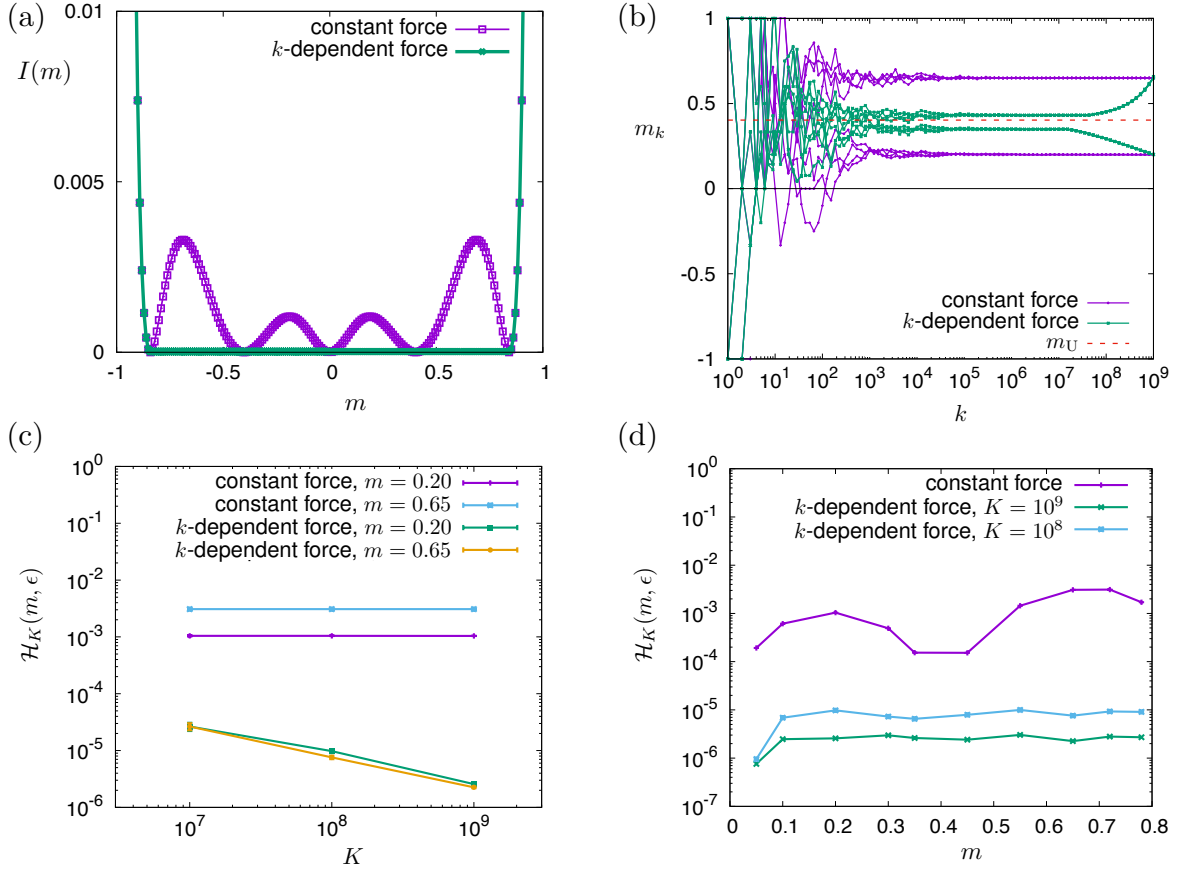


FIG. 5. Reversible growth model with $(c, J) = (5.0, 4.0)$, which is representative of the regime where the model has three steady states. (a) Bounds on the rate function in (12), obtained using control forces that are independent of k , and with k -dependent forces. Compare with Fig. 1. The data with $I(m) > 0$ are obtained by numerical minimisation of (47) but do not involve simulations of the growth process itself. (b) Trajectories of the controlled dynamics for $K = 10^8$, which achieve either $m_K \approx 0.2$ or $m_K \approx 0.65$. (c) Results for \mathcal{H}_K using these choices for the controlled dynamics. Data are shown for increasing K , analogous to Fig. 2(b). For the time-dependent control force, this bound decays as $K^{-1/2}$, consistent with (51). (d) The behaviour of \mathcal{H}_K as a function of m , analogous to Fig. 2(c). The decrease of \mathcal{H}_K with K occurs for all m within this range.

to obtain a controlled process with b as the steady state magnetisation. This minimisation fixes the parameter λ and hence also c' . We then use the steady state of this controlled process as an initial condition and solve (49,50) forwards in u , starting from an (arbitrary) initial value u_0 . The solution stops when the magnetisation hits the target. This happens at some $u = u_1$ and we set $u_1 = \log K$ so that the magnetisation will hit the target at the required time. This requires that we identify $k^* = \log u_0$ as the point when we remove the control forces and allow the system to start evolving according to (49,50). Hence $k^* = K e^{u_0 - u_1}$. Given the initial choice b , this yields a value for k^* such that the system with time-dependent control forces will hit the target m . The average action for this process is given by the product of (47) and k^* , which is straightforward to evaluate.

It remains to optimise the choice of b . By analogy with (25,26), we choose this parameter such that the average

action for the controlled process is

$$\langle \mathcal{A}/K \rangle_{\text{con}} \approx \frac{a_A}{\sqrt{K}}, \quad (51)$$

where a_A is a parameter of order unity (we take $a_A = 0.1$). Given a target m (with $|m| < m_S$) and a (sufficiently-large) value of K , it is possible to choose an initial guess for b such that (i) the left hand side of (51) is larger than the right hand side, and (ii) the left hand side is reduced by moving b closer to m_U . Then, one may move b towards m_U in suitably-chosen steps until one finds parameters (b, k^*) that solve (51). The method for computation of $\langle \mathcal{A} \rangle_{\text{con}}$ also fixes the values for (λ, c') , as described above.

In this procedure, there is only one pitfall, which is similar to the irreversible case: Eqs. (49,50) are only applicable if the distribution of m_{k^*} is sharply-peaked. (Specifically, its mean b should differ from m_U by an amount that is much larger than its standard deviation, which is of order $1/\sqrt{k^*}$). This requirement is always satisfied if

K is large enough.

Combining the ingredients, it follows that for large- K , we have established a bound on \mathcal{I}_K that scales as

$$\mathcal{H}_K(m, \epsilon) \simeq \frac{a_A}{\sqrt{K}}. \quad (52)$$

This bound tends to zero at large K . We emphasise that while this procedure for fixing b, k^* is numerical, it does not involve any simulation of the growth process, only minimisation of (47) and numerical solution of (49,50).

For cases where the model has two steady states, this method operates in the same way as the irreversible model and yields the same results. (The unstable fixed point has $m_U = 0$ in this case.) By (52) one has $\mathcal{H}_K(m, \epsilon) \rightarrow 0$ as $K \rightarrow \infty$ so the rate function in (12) reduces to $I(m) = 0$ for $|m| \leq m_S$. All details of this computation are very similar to the irreversible model: for reasons of brevity we do not show numerical results in this case.

The more interesting situation occurs when the model has three steady states. In this case we have performed simulations of the controlled process, in order to obtain bounds on \mathcal{I}_K . Results are shown in Fig. 5(b,c,d), following the procedure given above for determination of (b, k^*, λ, c') . The trajectories of the controlled process remain close to the unstable fixed point for $k < k^*$, and diverge from it at later times. Depending on the value of b , they may be attracted towards the fixed point at 0, or the one at m_S . In either case, the method yields results that are consistent with (52) and sufficient to establish that $\mathcal{I}_K(m, \epsilon) \rightarrow 0$ as $K \rightarrow \infty$. Hence $I(m) = 0$ whenever $|m| \leq m_S$, as in the irreversible case.

It would be interesting to investigate further the scaling of the probability density ρ_K for these values of m , as in Sec. III B. We anticipate similar results to that section, but a detailed analysis is beyond the scope of this work.

V. DISCUSSION

These models of cluster growth show rich and interesting behaviour, both for typical trajectories [22] and for large deviations [11]. They describe well-mixed clusters, in the sense that growth rates depend on the mean magnetisation and not, for example, the magnetisation near the boundary of the cluster. This often results in a self-averaging property, so that fluctuations are small when clusters are large. However, in cases where the deterministic dynamics has multiple fixed points (including unstable ones), large fluctuations are still possible, because trajectories may remain close to the unstable fixed point for large times, before eventually leaving it and converging (slowly) to a stable steady state. See Fig. 2(a) and Fig. 5(b).

At the level of large deviations, these trajectories are associated with large fluctuations and manifest in a rate function $I(m)$ that is zero whenever $|m| < m_S$, recall

Fig. 1. The probability to find a magnetisation in this range is not suppressed exponentially in K . For the irreversible model, we have shown in Sec. III B that these probabilities decay as power laws in K and we expect similar behaviour for the reversible model too.

We have also emphasised that the models are not ergodic and do not fit the classes considered by [7, 24]. They can be expressed as non-Markovian processes and analysed using methods from [20, 21]. As noted in those works, this can lead to complex behaviour, including rate functions with different speeds. That theory is fully consistent with the behaviour observed here.

It is also useful to recall the analogy between large deviation theory and equilibrium thermodynamics [7, 14, 18]. Within this framework, probabilities of individual trajectories (in d dimensions of space and 1 dimension of time) are analogous to configurations of equilibrium systems in $d + 1$ dimensions. The growth models have no spatial degrees of freedom so $d = 0$; this means that trajectories of the growth model are analogous to configurations of a one-dimensional Ising model, where s_k is interpreted as the k th spin in the chain. The energy of a configuration of this Ising model is

$$E(\mathbf{s}) = E_0 - \sum_{k=1}^K \log p_k(s_k | m_{k-1}) \quad (53)$$

with $\mathbf{s} = (s_1, s_2, \dots, s_K)$ and m_{k-1} given by (3); also E_0 is an arbitrary additive constant and the analogy requires that the temperature $T = 1$. Equ. (53) corresponds to an Ising model with long-ranged interactions, while the standard Markovian class of models would have only nearest-neighbour interactions.

Within this analogy, the rate function in the LDP corresponds to a free energy in the equilibrium system. This means that the results of Fig. 1 and Fig. 5(a) somewhat resemble a double-tangent construction, which would usually be associated with phase coexistence (it is equivalent to the Maxwell construction, see Sec. 4.7 of [40]). The analogy between dynamical large deviations and phase coexistence is discussed, for example, in [15, 37, 41]. The physical analogue of phase coexistence in dynamical trajectories may depend on system details, but one possibility is that trajectories that realise the rare event of interest show different behaviour in early-time and late-time regimes, as in Fig. 2A of [41] and Fig. 4B of [15].

In the growth models considered here, the analogy with equilibrium phase coexistence is not complete because of the long-ranged interactions in the Ising energy (53). From Fig. 2(a), one sees that the trajectories that realise the relevant rare events have qualitatively different behaviour in the early-time regime ($k < k^*$) and the late-time regime ($k > k^*$), similar to the behaviour for Markovian models [15, 41]. However the behaviour in the late-time regime is not at all stationary, for example the typical magnetisation m_k depends on k throughout the range $k^* < k < K$. This is contrary to the be-

haviour in Markovian models [15, 37, 41] where averages depend weakly on time *within* the late-time and early-time regimes, even if they differ strongly *between* these two regimes. For this reason, we prefer not to use the terminology of phases and phase coexistence to describe the behaviour shown in Fig. 1. Nevertheless, the behaviour of the rate function is the same as one would obtain from a double-tangent construction.

We also emphasise that while the rate functions for these growth models are never concave, the double-tangent construction does not hold generally in non-Markovian systems [42] nor even in Markovian systems on non-compact state spaces [43] – in such cases, the applicability of the double-tangent construction has to be tested on a case-by-case basis. This is similar to analysis of thermodynamic phase coexistence in systems with long-ranged interactions, where the applicability of the Maxwell construction depends on the decay of the interaction potential [44]. For the growth models considered here, we have shown that the construction is applicable.

Finally, we comment on the usefulness of the bound (17) for numerical estimation of small probabilities, as in [11, 25]. For parameters where there is no spontaneous symmetry breaking in these models, the bounds of KGGW (obtained with control forces that are constant in time) are accurate. Our results here confirm that suitable choices of the controlled dynamics can also make

this bound accurate in the regime where the symmetry is broken (see for example Fig. 4). However, construction of the relevant controlled dynamics in that case required detailed understanding of the dynamical behaviour of the model (including analytical estimates of the action). Our conclusion is that this method is only reliable if one already has a precise understanding of the mechanism by which the relevant rare events (large deviations) will occur. In this case, one may design a controlled process with this mechanism in mind. However, experience with a range of model systems (see for example Sec. 3.4 of [28]) indicates that it is difficult to predict suitable controlled dynamics, without prior theoretical analysis. If one evaluates the bound (17) using a controlled process does not fully account for the mechanism of the rare event, one may expect to obtain bounds that are not accurate estimates of the probabilities of interest.

ACKNOWLEDGMENTS

I would like to thank Steve Whitelam for many interesting discussions about growth models and numerical sampling methods. I am also grateful to Rosemary Harris and Hugo Touchette, and Juan P. Garrahan for useful discussions, including those related to LDPs in non-Markovian processes, and the possibility of optimal control forces that depend explicitly on time.

-
- [1] F. den Hollander, *Large deviations* (American Mathematical Society, Providence, RI, 2000).
 - [2] J. Lebowitz and H. Spohn, *J. Stat. Phys.* **95**, 333 (1999).
 - [3] T. Bodineau and B. Derrida, *Phys. Rev. Lett.* **92**, 180601 (2004).
 - [4] L. Bertini, A. De Sole, D. Gabrielli, G. Jona-Lasinio, and C. Landim, *Rev. Mod. Phys.* **87**, 593 (2015).
 - [5] J. Mehl, T. Speck, and U. Seifert, *Phys. Rev. E* **78** (2008).
 - [6] B. Derrida, *J. Stat. Mech.* **2007**, P07023 (2007).
 - [7] V. Lecomte, C. Appert-Rolland, and F. van Wijland, *J. Stat. Phys.* **127**, 51 (2007).
 - [8] J. Tailleur and J. Kurchan, *Nature Phys.* **3**, 203 (2007).
 - [9] J. P. Garrahan, R. L. Jack, V. Lecomte, E. Pitard, K. van Duijvendijk, and F. van Wijland, *Phys. Rev. Lett.* **98**, 195702 (2007).
 - [10] P. I. Hurtado, C. P. Espigares, J. J. del Pozo, and P. L. Garrido, *J. Stat. Phys.* **154**, 214 (2014).
 - [11] K. Klymko, P. L. Geissler, J. P. Garrahan, and S. Whitelam, *Phys. Rev. E* **97**, 032123 (2018).
 - [12] R. J. Harris and G. M. Schütz, *J. Stat. Mech.* **2007**, P07020 (2007).
 - [13] T. R. Gingrich, J. M. Horowitz, N. Perunov, and J. L. England, *Phys. Rev. Lett.* **116**, 120601 (2016).
 - [14] J. P. Garrahan, R. L. Jack, V. Lecomte, E. Pitard, K. van Duijvendijk, and F. van Wijland, *J. Phys. A* **42**, 075007 (2009).
 - [15] L. O. Hedges, R. L. Jack, J. P. Garrahan, and D. Chandler, *Science* **323**, 1309 (2009).
 - [16] J. K. Weber, R. L. Jack, C. R. Schwantes, and V. S. Pande, *Biophys. J.* **107**, 974 (2014).
 - [17] C. Maes and K. Netocny, *EPL* **82**, 30003 (2008).
 - [18] H. Touchette, *Phys. Rep.* **478**, 1 (2009).
 - [19] R. L. Jack and J. P. Garrahan, *Phys. Rev. E* **81**, 011111 (2010).
 - [20] R. J. Harris and H. Touchette, *J. Phys. A* **42**, 342001 (2009).
 - [21] R. J. Harris, *J. Stat. Mech.* **2015**, P07021 (2015).
 - [22] K. Klymko, J. P. Garrahan, and S. Whitelam, *Phys. Rev. E* **96**, 042126 (2017).
 - [23] R. G. Morris and T. Rogers, *J. Phys. A* **47**, 342003 (2014).
 - [24] R. Chétrite and H. Touchette, *Ann. Henri Poincaré* **16**, 2005 (2015).
 - [25] S. Whitelam, *Phys. Rev. E* **97**, 032122 (2018).
 - [26] D. Jacobson and S. Whitelam, *arXiv:1903.06098*.
 - [27] R. L. Jack and P. Sollich, *J. Phys. A* **47**, 015003 (2014).
 - [28] R. L. Jack and P. Sollich, *Eur. Phys. J.: Spec. Topics* **224**, 2351 (2015).
 - [29] R. L. Jack and P. Sollich, *Prog. Theor. Phys. Supp.* **184**, 304 (2010).
 - [30] M. C. Bañuls and J. P. Garrahan, *arXiv:1903.01570*.
 - [31] S. Whitelam, *Phys. Rev. E* **97**, 062109 (2018).
 - [32] R. Chétrite and H. Touchette, *J. Stat. Mech.* **2015**, P12001 (2015).
 - [33] W. H. Fleming, in *Recent Mathematical Methods in Dynamic Programming*, edited by I. C. Dolcetta, W. H. Fleming, and T. Zolezzi (Springer Berlin Heidelberg,

- Berlin, Heidelberg, 1985) pp. 52–66.
- [34] T. Nemoto, E. Fodor, M. E. Cates, R. L. Jack, and J. Tailleur, Phys. Rev. E **99**, 022605 (2019).
 - [35] T. Nemoto and S.-i. Sasa, Phys. Rev. Lett. **112**, 090602 (2014).
 - [36] T. Nemoto, F. Bouchet, R. L. Jack, and V. Lecomte, Phys. Rev. E **93**, 062123 (2016).
 - [37] T. Nemoto, R. L. Jack, and V. Lecomte, Phys. Rev. Lett. **118**, 115702 (2017).
 - [38] U. Ray, G. K.-L. Chan, and D. T. Limmer, Phys. Rev. Lett. **120**, 210602 (2018).
 - [39] G. Ferré and H. Touchette, J. Stat. Phys. **172**, 1525 (2018).
 - [40] K. Huang, *Introduction to Statistical Physics*, 2nd ed. (CRC press, Boca Raton, FA, 2010).
 - [41] Y. S. Elmatad, R. L. Jack, D. Chandler, and J. P. Garrahan, Proc. Natl. Acad. Sci. USA **107**, 12793 (2010).
 - [42] K. R. Duffy and A. Sapozhnikov, J. Appl. Probab. **45**, 107 (2008).
 - [43] D. Nickelsen and H. Touchette, Phys. Rev. Lett. **121**, 090602 (2018).
 - [44] A. Campa, T. Dauxois, and S. Ruffo, Phys. Rep. **480**, 57 (2009).